Bahareh Nateghi and Christoph Janiak*

Synthesis and characterization of two bifunctional pyrazole-phosphonic acid ligands

https://doi.org/10.1515/znb-2019-0170
Received October 24, 2019; accepted November 4, 2019

Abstract: The bifunctional compounds 3,5-dimethyl-4-(4-phosphonophenyl)-1*H*-pyrazole **1** and 4-(4-phosphonophenyl)-1*H*-pyrazole **2** were synthesized via Suzuki-Miyaura coupling, starting from a Boc-protected pyrazolylboronic acid ester and the iodoarylphosphonate. The target compounds were isolated after acidic hydrolysis in the form of the hydrochloride salts **1** · HCl and **2** · HCl · H_2O with a yield of 81% and 86%, respectively. $Pd(dppf)Cl_2$ was found to be superior to $Pd(PPh_3)_4$ as a catalyst; dry 1,4-dioxane as a solvent, Cs_2CO_3 as a base, and no co-ligands were the best found conditions. The alternative routes through iodoarylphosphonate of iodoarylpyrazole, with the crucial steps based on the copper-catalyzed coupling with acetylacetone or the Arbuzov reaction were proven inefficient. The structures of the isolated hydrochloride salts **1** · HCl and **2** · HCl · H_2O feature hydrogen-bonded networks involving the chloride anions.

Keywords: bifunctional ligands; hydrogen bond; phosphonate; pyrazolate; Suzuki-Miyaura.

1 Introduction

The development of new ligand classes is crucial for the progress of the field of coordination polymers (CPs) and, in particular, its most important sub-field of metal-organic frameworks (MOFs). The increase of the stability and the tuning of structural characteristics of CPs/MOFs are important for various potential applications, including catalysis, gas storage and separation, sensing and heat transformation [1–4]. In recent years, many types of polytopic organic ligands with different donor groups, such as carboxylate, pyridyl, sulfonate, amine, etc., have been used for the synthesis of MOFs, with the most important and numerous class being the carboxylate compounds [5]. The far less numerous, but very promising azolate, especially pyrazolate, as well as phosphonate MOFs are the main competitors in terms of thermal and chemical, particularly hydrolytic stability [6, 7]. ZIF-8 [Zn(2-methylimidazolate)$_2$] [8–10] is one of the most hydrolytically stable azolate-based MOFs, and has been demonstrated to be extremely stable in boiling water over a broad pH range. Pyrazolate-based metal units often possess unsaturated metal centres and feature heterogeneous catalytic properties, like MFU-1 [Co_4O(3,5-dimethylpyrazolate)$_6$], and MFU-2 [Co_4O(bdpb)$_3$] (H_2-bdpb = 1,4-bis[3,5-dimethyl)-pyrazol-4-yl]benzene) [11] both of which contain redox-active Co^{2+} centres. Moreover, coordination polymers and MOFs based on pyrazolate are interesting for potential applications such as heat transformation, magnetism, gas separation, etc. [12–16]. Phosphonate MOFs with proven porosity are still an emerging area with a relatively limited results, which are, though, very important, due to their typically high stability. The scarcity of the results might be explained by the propensity of the phosphonates to form layered structures. The polymorphism, typical for multidentate ligands, and low-reversibility of metal-ligand bond formation, which hinders the isolation of good-quality single-crystals, further complicate the synthesis and investigation of porous metal-phosphonate networks [17, 18]. Clearfield et al. have done extensive work to prepare a series of mesoporous metal phosphonate frameworks with 1,4-phenylenediphosphonate and biphenyldiphosphonate as ligands and zirconium as the metal atom [19]. Wharmby et al. reported a series of isoreticular compounds based on the linkers *N*,*N*′-piperazinediphosphonate and *N*,*N*′-bispiperidinediphosphonate with Ni and Co as metal atoms, which are porous to N_2 with a pore volume of up to 0.68 $cm^3\ g^{-1}$ [20]. More recently, the sorption properties of M-CAU-29 (M=Ni, Mn, Co and Cd), having a porphyrin-based tetraphosphonate linker, were studied [21]. Ni-CAU-29 shows no uptake of N_2 at $T = 77$ K, but a water uptake of 181 mg g^{-1} at 298 K. Mn-, Co- and Cd-CAU-29 show N_2 uptakes of 90, 145 and 180 $m^2\ g^{-1}$ and H_2O uptakes of 140, 166 and 116 mg g^{-1}, respectively. Further, Ni-metallated porphyrin-based tetraphosphonates with Zr and Hf atoms as metal nodes (Zr- and

***Corresponding author: Christoph Janiak,** Institut für Anorganische Chemie und Strukturchemie, Heinrich-Heine-Universität Düsseldorf, Universitätsstraße 1, D-40225 Düsseldorf, Germany,
Tel.: +49-211-81-12286, E-mail: janiak@uni-duesseldorf.de
Bahareh Nateghi: Institut für Anorganische Chemie und Strukturchemie, Heinrich-Heine-Universität Düsseldorf, Universitätsstraße 1, D-40225 Düsseldorf, Germany

Hf-CAU-30) demonstrated high specific surface areas of 1070 and 1030 $m^2 g^{-1}$, respectively [22].

The use of the mixed-functional ligands is an approach to combine the advantages of different types of coordination groups and to use them synergistically in the structural context [23, 24]. The pyrazolate and phosphonate pair is especially interesting, allowing to target both single- and bimetal species. Indeed, both the pyrazolate and phosphonate ligands are effectively coordinated by divalent transition metal ions. However, the pyrazolate anion is more affine to 'softer' metal ions (e.g. Cu^{2+}, Zn^{2+}), while the oxygen-donating phosphonate group prefers 'hard' metal ions (e.g. Fe^{3+}, Zr^{4+}) in the HSAB [25] concept, which would allow for the targeted bimetal approach. Mixed pyrazolate/phosphonate MOFs are yet practically unknown. However, existing mixed-ligand CPs with versatile architectures [26, 27], with a combination of (organo)phosphonate groups [28, 29] together with separate pyrazolate ligands, prove the viability of the concept. Besides, high chemical and thermal stabilities could also be expected as in the already more advanced CPs with mixed-functional carboxylate-pyrazolate [13, 30] or carboxylate-phosphonate linkers [31].

In this work, we have developed the synthesis of bi- or mixed-functional pyrazole-phosphonic acid molecules based on a *p*-phenylene core, which should be primary targets as MOF ligands. To the best of our knowledge, 3,5-dimethyl-4-(4-phosphonophenyl)-1*H*-pyrazole and 4-(4-phosphonophenyl)-1*H*-pyrazole (Schemes 1 and 2) are unknown so far, possibly because their low-cost large-scale preparation is problematic, as is shown below.

2 Results and discussion

Our strategy was to use the 1,4-diiodobenzene as a starting compound and to substitute the iodine atoms sequentially by pentane-2,4-dion-3-yl (i.e. acetylacetonyl, as a 3,5-dimethylpyrazole synthon) and diethylphosphonyl groups in either order. This route should potentially allow the preparation of the target compounds on a large scale at low cost.

In the first attempted sequence, 3-(4-iodophenyl)-2,4-pentadione was prepared according to a method of Liu et al. [32], starting from 1,4-diiodobenzene and acetylacetone in the presence of CuI/L-proline as catalyst (Scheme 1a). This intermediate and hydrazine monohydrate were dissolved in deionized water to afford the respective 3,5-dimethylpyrazole, following a known procedure by Spassow [33]. However, the next step to synthesize the phosphonate ester through the nickel(II) catalyzed conversion was not successful. The NH-pyrazole is evidently not inert under the conditions of the Michaelis-Arbuzov reaction, which proceeds at high temperature (note, that under these conditions the acetylacetonyl precursor is expected to be even less inert).

In the reverse sequence (Scheme 1b), the diethyl 4-iodophenylphosphonate was synthesized in the first step, followed by a conversion attempt to diethyl-4-(pentane-2,4-dion-3-yl)phenylphosphonate. A mixture of products was obtained and the purification trials, including column chromatography, were not successful.

The failure of stepwise introduction of functionalities prompted us to turn to the Suzuki-Miyaura cross-coupling reaction between components already containing the necessary functionalization (Scheme 2). Commercially

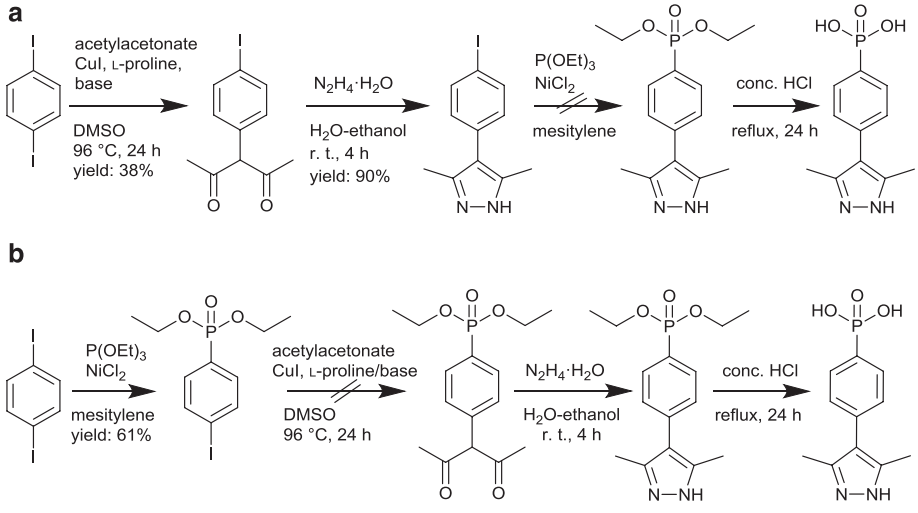

Scheme 1: Potential, but unsuccessful routes towards 3,5-dimethyl-4-(4-phosphonophenyl)-1*H*-pyrazole, **1** starting from 1,4-diiodobenzene.

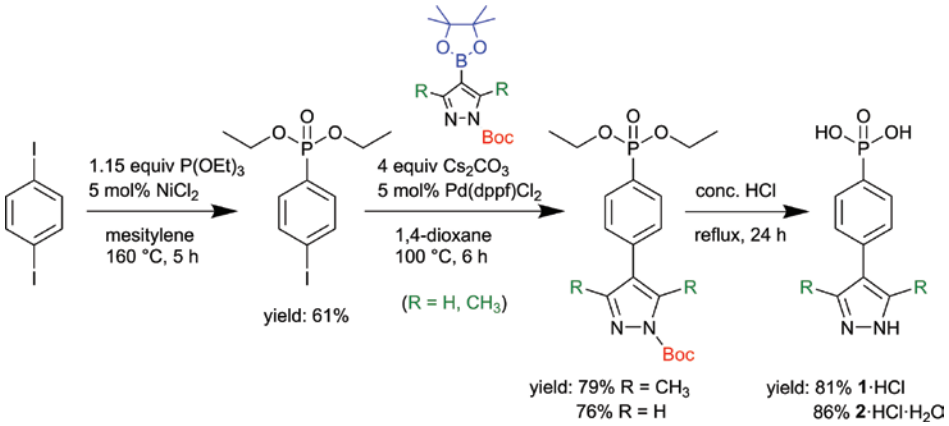

Scheme 2: Reaction sequence for the successful synthesis of **1** · HCl and **2** · HCl · H_2O starting from 1,4-diiodobenzene.

available pinacol esters of the 1-Boc-3,5-dimethylpyrazole-4-boronic acid or 1-Boc-pyrazol-4-boronic acids (Boc stands for *N-tert*-butyloxycarbonyl) were used as the pyrazole containing reactants, and the synthesized diethyl 4-iodophenylphosphonate as the phosphonate containing one. Our analysis of the literature indicated that while 1*H*-pyrazoles could participate in the Suzuki-Miyaura coupling, both the number of steps and the yields are lower compared to the cases when N-protected pyrazoles are used. Pd(dppf)Cl_2 as a catalyst demonstrated higher efficiency compared to Pd(PPh_3)$_4$, and performed well in dry 1,4-dioxane at $T = 100$°C for 6 h, in the presence of Cs_2CO_3 as a base [34]. The bifunctional pyrazole-phosphonic acid was obtained through the hydrolysis of the obtained esters, thus liberating the phosphonic acid and the 1*H*-pyrazole groups.

Thus, 3,5-dimethyl-4-(4-phosphonophenyl)-1*H*-pyrazole, **1**, and 4-(4-phosphonophenyl)-1*H*-pyrazole, **2**, were synthesized via coupling and subsequent hydrolysis. The products were isolated in the form of the hydrochlorides **1** · HCl and **2** · HCl · H_2O in overall yields of 32% and 33%, respectively (Scheme 2).

Colorless needle-like crystals of **1** · HCl and **2** · HCl · H_2O were obtained by slow evaporation of hydrochloric acid solutions of **1** and **2**. The phase purities of the bulk samples were verified by comparison of the powder X-ray diffraction patterns with the simulations from the obtained single crystal X-ray data sets (Fig. S8 and Fig. S17; Supporting information available online).

Compound **1** · HCl crystallizes in the monoclinic space group $P2_1/c$ the co-crystallizing molecule hydrochloric acid protonating the pyrazole group to a pyrazolium cation (Fig. 1a). The structure of **1** · HCl can be dissected into hydrogen-bonded chains of centrosymmetric $(\cdots {}^{+}HAB \cdots BAH^{+} \cdots 2Cl^{-})_n$ aggregates of the bifunctional pyrazolium-phosphonic acid or $^{+}$HAB molecules (Fig. 1b). Two pyrazolium moieties and two chloride ions are associated in a 10-membered $\{\text{-pz}H^{+} \cdots Cl^{-}\}_2$ hydrogen-bonded ring motif, sustained by two strong charge-assisted $NH^{+} \cdots Cl^{-}$ hydrogen bonds. The two NH $\cdots$ Cl distances are slightly different with 3.060(2) and 3.169(2) Å, but are within the expected range of 3.05–3.2 Å for comparable $NH^{+} \cdots Cl^{-}$ cases [35]. The observed ring motif has a graph set descriptor of $R_4^2(10)$ [36], which is typically seen in structures of pyrazolium salts with halide anions [37]. The phosphonic acid groups are also associated pairwise, forming simple $\{RPO(OH)_2\}_2$ rings with a $R_2^2(8)$ graph set notation. This simple and symmetric association mode, well-known for carboxylic acids, is common for compounds containing a similar 1:1 donor/acceptor XO(OH) fragment (X=C, P, S) [38]. The $\{RPO(OH)_2\}_2$ ring is planar and built by strong O–H $\cdots$ O bonds, with a typical O $\cdots$ O distance of 2.546(2) Å [39]. The additional P–OH donor of the phosphonic acid group, which is not involved in the formation of the ring pattern, forms a strong hydrogen bond with the chloride anion of a neighboring hydrogen-bonded chain, $d(O \cdots Cl) = 2.976(2)$ Å (Fig. 1c). The $(\cdots {}^{+}HAB \cdots BAH^{+} \cdots 2Cl^{-})_n$ chains are, thereby, associated into sheets, which in turn are held together by weaker interactions, among which very weak methyl-CH $\cdots$ O and methyl-CH $\cdots$ Cl^{-} contacts are discernible.

The chains within the stacks are not planar and hence are not packed tightly to have a possible additional stabilization from $\pi \cdots \pi$ interactions. The latter would be typical for planar chains in bipyrazolium salts [37]. Two factors lead to the non-planarity: the $\{RPO(OH)_2\}_2$ ring pattern is not co-planar to that of the phenyl group due to the tetrahedral environment of the phosphorus atom and the phenyl ring is not coplanar with the pyrazole ring. The latter deviation is due to repulsion of the methyl groups of

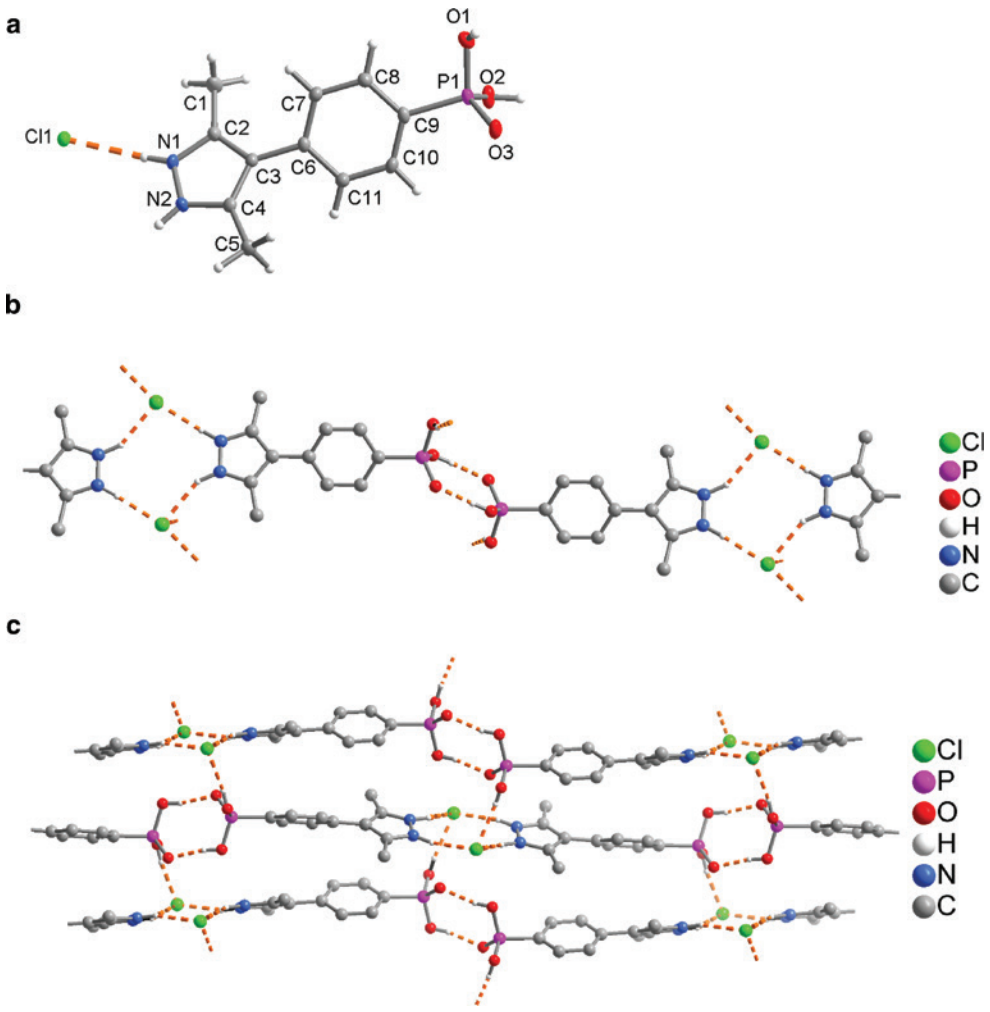

Fig. 1: (a) Asymmetric unit (50% displacement ellipsoids), (b) chain sub-structure and (c) two-dimensional hydrogen-bonded network of **1** · HCl. Details of the hydrogen-bonding interactions (orange dashed lines) are given in Table 2.

the pyrazole ring and the hydrogen atoms on the phenyl group. The dihedral pyrazole-phenyl angle is ~37.5°.

Compound **2** · HCl · H_2O crystallizes in the monoclinic space group $P2_1/c$. The structure incorporates also a water molecule of crystallization (Fig. 2a) to give the crystallographic formula **2** · HCl · H_2O. Again, the hydrochloric acid molecule protonates the pyrazole group to a pyrazolium cation. The water molecule perturbs the expected simple chain association which was seen in the structure of **1** · HCl (Fig. 2b). The water molecule is held by hydrogen bonding from an N–H donor and to a Cl^- and O(3) = P acceptor. Each Cl^- anion interacts with three H atoms (Fig. 2b), one from pzH^+, one from an H atom of {$(RPO(OH)_2)$} and one from an H atom of the water molecule. The crystal structure shows a hydrogen-bonded network with head-to-tail linked pyrazolium-phosphonic acid or $^+$HAB molecules via the N–H···Cl^- hydrogen bonds between the $-N_2H_2^+$ and $-PO_3H_2$ moieties. Compound **2** · HCl · H_2O displays an overall three-dimensional supramolecular structure, which consists of strong charge-assisted OH···Cl^-, NH^+···Cl^-, plus OH···O and weak CH···Cl^- hydrogen bonds (Fig. 2b). The phenyl and pyrazolium rings are not coplanar but form a dihedral angle of 11.37(7)°.

The thermogravimetric behavior of **1** · HCl shows a weight loss of 11.3% between $T = 150$ and 250°C, which corresponds to the one molecule of hydrogen chloride (12.5% theoretically) (Fig. 3). The mass loss of ~5% in the range of 250 and 350°C is assigned to the dehydration (–1 H_2O, 7% theoretically) through the condensation of phosphoric acid groups to give anhydrides [40].

The themogravimetric behavior of **2** · HCl · H_2O in Fig. 4 shows a weight loss of 5.3% between $T = 60$ and 150°C corresponding to the one molecule of water (6.1% theoretically). The second step of 8.4% in the temperature range of 150–320°C is assigned to the one molecule of hydrogen chloride (14.2% theoretically).

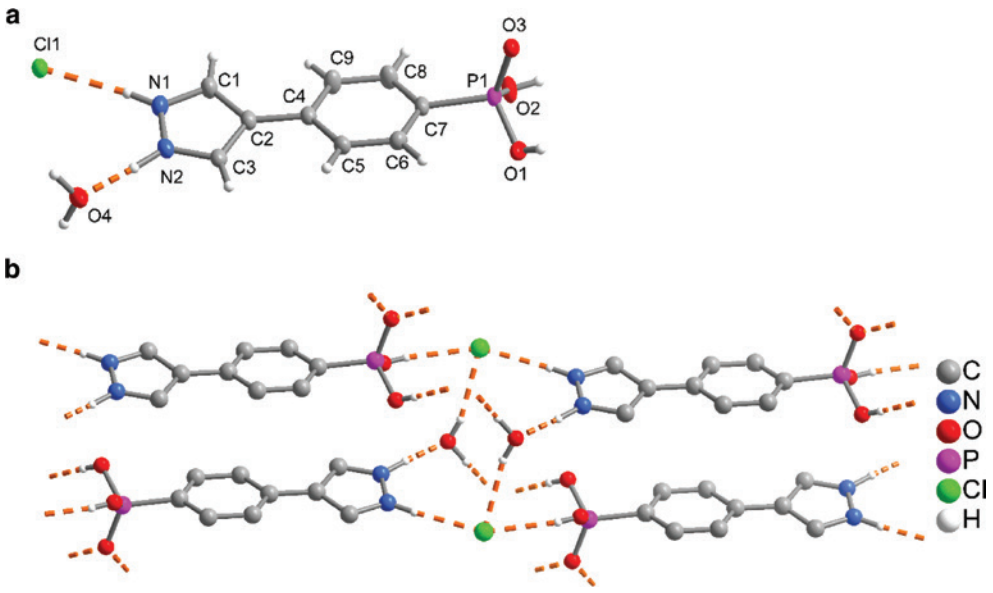

Fig. 2: (a) Asymmetric unit (50% displacement ellipsoids) and (b) section of the three-dimensional hydrogen-bonded network of **2** · HCl · H_2O. Details of the hydrogen-bonding interactions (orange dashed lines) are given in Table 3.

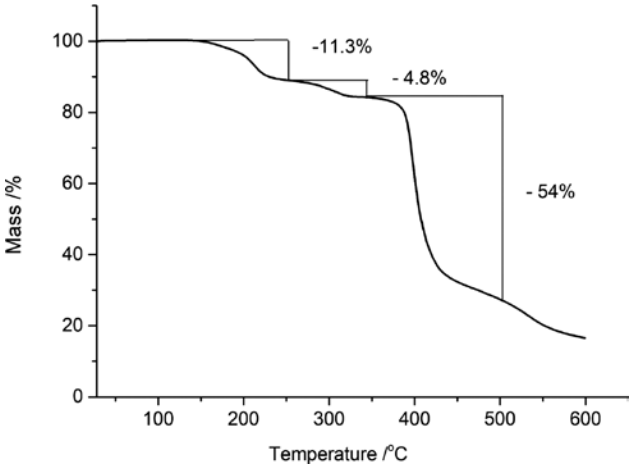

Fig. 3: TGA diagram of **1** · HCl in the temperature range 27–600°C with a heating rate of 5 K min^{-1} under N_2 atmosphere.

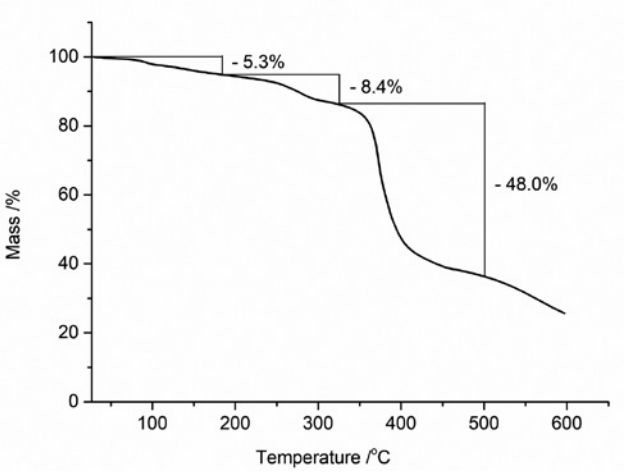

Fig. 4: TGA diagram of **2** · HCl · H_2O in the temperature range 27–600°C with a heating rate of 5 K min^{-1} under N_2 atmosphere.

3 Experimental section

3.1 Materials and measurements

All reagents and starting materials were commercially available and used without further purification. Elemental analyses were performed on a Perkin Elmer CHN 2400 (Perkin Elmer, Waltham, MA, USA). ^{1}H, ^{13}C, ^{31}P NMR spectra were collected with a Bruker Avance DRX-300 or Bruker Avance DRX-600 instrument. FT-IR spectra were recorded in ATR mode on a Bruker TENSOR 37 IR spectrometer (Bruker Optics, Ettlingen, Germany). The absorbance bands are presented by using of the following abbreviations: strong (s), medium (m), weak (w), broad (br) and shoulder (sh). The powder X-ray diffraction patterns (PXRD) were recorded using a Bruker AXS D2 Phaser with a flat silicon low background sample holder, using Cu$K\alpha$ radiation with $\lambda = 1.5418$ Å at 30 kV, 10 mA and a Lynxeye 1D detector. The measurement was performed at room temperature with 2θ angles in the range 5–50° and a step size of 0.02° (in 2θ). Thermogravimetric analysis data (TGA) was collected on a Netzsch TG 209 F3 Tarsus instrument (Netzsch, Selb, Germany) equipped with an aluminum crucible and using a heating rate of 5 K min^{-1} in air.

3.2 Synthesis of 3,5-dimethyl-4-(4-phosphonophenyl)-1*H*-pyrazole, 1 · HCl

3.2.1 Synthesis of diethyl 4-iodophenylphosphonate

In a two necked 50 mL flask 3.0 g (0.009 mol) of 1,4-diiodobenzene and 0.059 g (0.0004 mol) of anhydrous $NiCl_2$ were suspended in 10 mL of mesitylene. The suspension was placed under nitrogen and heated to 160°C with refluxing. After 1 h 1.74 g (0.01 mol) of triethyl phosphite was added dropwise over 2 h. After refluxing for another 2 h for completion of the reaction, the yellow suspension was allowed to cool to the room temperature. The yellow mixture was filtered to remove the rest of nickel salt, washed with hexane and heated to 130°C to remove mesitylene. The excess of solvent was removed under reduce pressure. The yellow residue was subjected to column chromatography (silica gel, 1:1 ethyl acetate:hexane). The resulting liquid was dried under reduce pressure to afford 1.83 g (61%) of pure product. – ^{1}H NMR (300 MHz, $CDCl_3$): δ (ppm) = 1.31 (t, 6H), 4.11 (q, 4 H), 7.51 (d, 2H), 7.82 (d, 2H) (Fig. S1). – ^{13}C NMR (300 MHz, DMSO-d_6): δ (ppm) = 16.94 (CH_3), 62.88 (CH_2), 127.38 (O–CH_3), 129.9 (O–CH_3), 133.80–138.39 (aromatic C atoms) (Fig. S2). – ^{31}P{H} NMR (300 MHz, DMSO-d_6): δ (ppm) = 18.05 (Fig. S3).

3.2.2 Synthesis of 3,5-dimethyl-4-(4-phosphonophenyl)-1-*tert*-butoxycarbonyl-pyrazole

According to the Suzuki-Miyaura cross-coupling reaction [41], 1.0 g (0.003 mol) of diethyl 4-iodophenylphosphonate, 1.1 g (0.004 mol) of 3,5-dimethylpyrazole-4-boronic acid pinacol ester, and 3.9 g (0.012 mol) of Cs_2CO_3 were placed in a two necked 250 mL flask under nitrogen and suspended in 100 mL of 1,4-dioxane. Finally, 0.122 mg (0.15 mmol) of Pd(dppt)Cl_2 was added under constant stirring. The suspension was heated to 100°C for 6 h. After the reaction was completed as monitored by TLC, the cooled dark beige suspension was filtered and subjected to column chromatography (silica gel, 97: 3% ethyl acetate-methanol) to yield 0.76 g (76%) of pure oily product. – ^{1}H NMR (600 MHz, $CDCl_3$): δ (ppm) = 1.35 (t, 6H), 1.66 (m, 9H), 2.26 (s, 3H), 2.46 (s, 3H), 4.19 (q, 4H), 7.32 (d, 2H), 7.84 (d, 2H) (Fig. S4). – ^{13}C NMR (600 MHz, $CDCl_3$): δ (ppm) = 16.75 (CH_3), 28.42 (CH_3), 62.59 (CH_3), 85.74 (CH_2) 136.83 (s, C–N), 140.70 (C–O), 148.89–150.69 (aromatic C atoms) (Fig. S5). – ^{31}P{H} NMR (600 MHz, $CDCl_3$): δ (ppm) = 18.61 (Fig. S6).

3.2.3 Synthesis of 3,5-dimethyl-4-(4-phosphonophenyl)-1*H*-pyrazole, 1 · HCl

In a 15 mL Pyrex tube 0.76 g (0.002 mol) of 3,5-dimethyl-4-(4-phosphonophenyl)-1-*tert*-butoxycarbonyl-pyrazole was dissolved in 3.0 mL of concentrated HCl and heated to 100°C for 24 h. A colourless crystalline product was obtained, which was dried in air (Fig. S7). Yield 0.61 g (81%). m.p. >350°C, decomp. >400°C. Elemental analysis calcd. (%) for $C_{11}H_{14}N_2O_3PCl$: C 45.77, N 9.70, H 4.89; found C 44.25, N 9.75, H 3.43. – FT-IR ATR (neat): ν_{max} (cm^{-1}) = 2708 (br), 1595 (w), 1203 (s), 1139 (s), 981 (s), 914 (s), 835 (s), 603 (s) (Fig. S9). – ^{1}H NMR (300 MHz, NaOD, DMSO-d_6): δ (ppm) = 2.24 (s, 6H), 7.23 (m, 2H), 7.68 (m, 2H) (Fig. S10). – ^{13}C NMR (300 MHz, NaOD, DMSO-d_6): δ (ppm) = 12.91 (CH_3), 115.45 (C–N), 127–144.60 (aromatic C atoms) (Fig. S11). – ^{31}P{H} NMR (300 MHz, NaOD, DMSO-d_6): δ (ppm) = 12.48 (Fig. S12).

3.3 Synthesis of 4-(4-phosphonophenyl)-1*H*-pyrazole, 2 · HCl · H_2O

3.3.1 Synthesis of 4-(4-phosphonophenyl)-1-*tert*-butoxycarbonyl-pyrazole

In a two necked 250 mL flask 1.0 g (0.003 mol) of diethyl 4-iodophenylphosphonate, 1.04 g (0.004 mol) of 1-Boc-pyrazol-4-boronic acid pinacol ester and 3.8 g (0.012 mol) of Cs_2CO_3 were placed under nitrogen and suspended in 100 mL of 1,4-dioxane. Finally, 0.12 mg (0.15 mmol) of Pd(dppt)Cl_2 was added under constant stirring. The suspension was heated to 100°C for 6 h. After the reaction was completed as monitored by TLC, the cooled dark beige suspension was filtered and subjected to column chromatography (silica gel, 97: 3% ethyl acetate-methanol) to yield 0.79 g (79%) of pure oily product. – ^{1}H NMR (300 MHz, $CDCl_3$): δ (ppm) = 1.33 (t, 3H), 1.68 (s, 9H), 4.15 (m, 4H), 7.61 (m, 2H), 7.80 (m, 2H), 8.03 (s, 1H), 8.38 (s, 1H) (Fig. S13). – ^{13}C NMR (300 MHz, $CDCl_3$): δ (ppm) = 16.34 (CH_3), 24.54 (CH_3), 62.27 (CH_3), 86.0 (CH_2), 125.75 (s, C–N), 127.21 (C–O), 141.65 (aromatic C atoms) (Fig. S14). – ^{31}P{H} NMR (300 MHz, $CDCl_3$): δ (ppm) = 13.03 (Fig. S15).

3.3.2 Synthesis of 4-(4-phosphonophenyl)-1*H*-pyrazole, 2 · HCl · H_2O

In a 15 mL Pyrex tube 0.79 g (0.002 mol) of 4-(4-phosphonophenyl)-1-*tert*-butoxycarbonyl-pyrazole was dissolved in 3.0 mL of concentrated HCl and heated

Table 1: Crystal data and structure refinement for **1** · HCl and **2** · HCl · H_2O.

	1 · HCl	**2** · HCl · H_2O
Empirical formula	$C_{11}H_{14}N_2O_3PCl$	$C_9H_{12}N_2O_4PCl$
M_r/g mol^{-1}	288.66	278.63
T/K	100(2)	100(2)
Wavelength/Å	1.54178	1.54178
Crystal system	Monoclinic	Monoclinic
Space group	$P2_1/c$	$P2_1/c$
a/Å	9.5963(19)	7.8070(5)
b/Å	7.7811(16)	12.6042(8)
c/Å	17.424(4)	12.3523(8)
β/deg	95.52(3)	90.595(2)
V/Å^3	1295.0(5)	1215.41(13)
Z	4	4
Calcd. density/g cm^{-3}	1.48	1.52
μ/mm^{-1}	3.8	4.1
F(000)/e	600	576
Crystal size/mm^3	0.4 × 0.2 × 0.1	0.4 × 0.1 × 0.05
θ range/deg	4.629–68.021	5.013–66.653
Reflections collected	14 605	16 599
Independent reflections; R_{int}	2327; 0.0477	1241; 0.0371
Completeness to θ_{max}/%	99.0	99.7
Data; ref. parameters	2327; 219	2141; 202
Goodness-of-fit	1.003	1.059
$R1$; $wR2$ (all data)	0.0379; 0.1075	0.0310; 0.0869
$\Delta\rho_{fin}$ (max; min), e Å^{-3}	0.595; −0.537	0.536; −0.312

to 100°C for 24 h. A colourless crystalline product was obtained, which was dried in air (Fig. S16). Yield 0.68 g (86%). m.p. >300°C, decomp. >350°C. – Elemental analysis calcd. (%) for $C_9H_{12}N_2O_4PCl$: C 38.80, N 10.05, H 4.34; found C 38.88, N 10.96, H 4.10. – FT-IR ATR (neat): ν_{max} (cm^{-1}): 3120 (v), 1682 (w), 1607 (w), 1139 (s), 1050 (s), 992 (s), 926 (s), 827 (s), 741 (s), 572 (s) (Fig. S18). – ^{1}H NMR (600 MHz, NaOD, DMSO-d_6): δ (ppm) = 7.65 (m, 2H), 7.70 (m, 2H), 8.17 (s, 1H) (Fig. S19). – ^{13}C NMR (600 MHz, NaOD, DMSO-d_6): δ (ppm) = 123.76 (C–N), 130–136 (aromatic C atoms) (Fig. S20). – ^{31}P{H} NMR (600 MHz, NaOD, DMSO–d_6): δ (ppm) = 12.96 (Fig. S21).

3.4 Single crystal X-ray diffraction

Selected needle-like single crystals of suitable optical quality of **1** · HCl and **2** · HCl · H_2O selected under a polarizing microscope and coated in perfluorinated oil were mounted on a 0.2 mm cryo loop and transferred to the diffractometer, a Bruker Kappa APEX2 CCD X-ray diffractometer system (Bruker AXS Inc., Madison, WI, USA) with microfocus tube, Cu$K\alpha$ radiation (λ = 1.54178 Å), 100 ± 2 K; multilayer mirror system, ω scans; data collection with Apex2 [42], cell refinement with Smart and data reduction with Saint [43], experimental absorption correction with Sadabs [44]. The information regarding data collection and structure refinement is summarized in Table 1. The structures were solved by Direct Methods using ShelxL2016 [45, 46] and refined by full-matrix least-squares on F^2 using Shelx-97. Graphics were drawn with Diamond [47].

Table 2: Details of the hydrogen-bonding interactions in **1** · HCl.

***D*–H···*A*[a]**	***D*–H/Å**	**H···*A*/Å**	***D*···*A*/Å**	***D*–H···*A*/deg**	**Symmetry transformations**
N1–H1···Cl1	0.83(3)	2.24(3)	3.060(2)	170(2)	
O1–H1···Cl1^{i}	0.85(4)	2.13(4)	2.976(2)	170(3)	i = $x-1, -y+1/2, z-1/2$
N2–H2···Cl1^{ii}	0.82(3)	2.40(3)	3.169(2)	157(3)	ii = $-x+2, -y+1, -z+2$
O2–H2···O3^{iii}	0.81(3)	1.74(3)	2.546(2)	172(3)	iii = $-x, -y+1, -z+1$
C1–H1B···O1^{iv}	0.95(3)	2.60(3)	3.388(3)	140(2)	iv = $-x+1, -y+1, -z+1$
C5–H5A···Cl1^{v}	1.01(3)	2.86(3)	3.692(2)	141(2)	v = $x-1, y, z$

[a]D, Donor; A, acceptor.

Table 3: Details of the hydrogen-bonding interactions in **2** · HCl · H_2O.

***D*–H···*A*[a]**	***D*–H/Å**	**H···*A*/Å**	***D*···*A*/Å**	***D*–H···*A*/deg**	**Symmetry transformations**
N1–H1···Cl1	0.89(3)	2.23(3)	3.1092(16)	169(2)	
N2–H2···O4	0.98(2)	1.61(2)	2.5871(18)	176(2)	
O1–H1···O3^{i}	0.65(3)	1.88(3)	2.5324(17)	176(3)	i = $-x+1, -y+1, -z$
O2–H2···Cl1^{ii}	0.75(3)	2.31(3)	3.0491(14)	171(2)	ii = $x-1, y, z-1$
O4–H4···Cl1^{iii}	0.81(3)	2.31(3)	3.0881(13)	163(2)	iii = $-x+2, -y+1, -z+2$
O4–H3···O3^{iv}	0.89(3)	1.82(3)	2.6786(16)	161(3)	iv = $-x+2, -y+1, -z+1$

[a]D, Donor; A, acceptor.

CCDC 1961142 and 1961143 contain the supplementary crystallographic data for **1** · HCl and **2** · HCl · H_2O, respectively. These data can be obtained free of charge from The Cambridge Crystallographic Data Centre via www.ccdc.cam.ac.uk/data_request/cif.

4 Conclusions

In summary, two novel bifunctional pyrazolate-phosphonate ligands 3,5-dimethyl-4-(4-phosphonophenyl)-1*H*-pyrazole, **1** and 4-(4-phosphonophenyl)-1*H*-pyrazole, **2** have been prepared via a Suzuki-Miyaura cross-coupling and their crystal structures determined. These multidentate ligands with five potential coordination sites offer the use as suitable organic spacers to provide new coordination polymers or metal-organic frameworks (MOFs). The high thermal stability of the synthesized compounds aids in the hydrothermal synthesis of coordination polymers or MOFs. We are confident that in continuation of this work a large number of interesting supramolecular complexes for a variety of applications will be reported in the future.

5 Supporting information

PXRD patterns, ^{1}H, ^{13}C, ^{31}P NMR and IR spectra are given as supplementary material available online (DOI: 10.1515/znb-2019-0170).

Acknowledgements: The authors thank Dr. Ishtvan Boldog for his kind support during this project.

References

[1] C. Janiak, *Dalton Trans*. **2003**, 2781–2804.
[2] S. Kitagawa, R. Kitaura, S. I. Noro, *Angew. Chem. Int. Ed*. **2004**, *43*, 2334–2375.
[3] A. H. Chughtai, N. Ahmad, H. A. Younus, A. Laypkovc, F. Verpoort, *Chem. Soc. Rev.* **2015**, *44*, 6804–6849.
[4] J. R. Li, R. J. Kuppler, H. C. Zhou, *Chem. Soc. Rev.* **2009**, *38*, 1477–1504.
[5] S. Natarajan, P. Mahata, *Curr. Opin. Solid State Mater. Sci.* **2009**, *13*, 46–53.
[6] G. Alberti, M. Casciola, U. Costantino, R. Vivani, *Adv. Mater.* **1996**, *8*, 291–303.
[7] A. Clearfield, *Dalton Trans.* **2008**, 6089–6102.
[8] X. C. Huang, Y. Y. Lin, J. P. Zhang, X. M. Chen, *Angew. Chem. Int. Ed.* **2006**, *45*, 1557–1559.
[9] K. S. Park, Z. Ni, A. P. Cote, J. Y. Choi, R. Huang, F. J. Uribe-Romo, H. K. Chae, M. O'Keeffe, O. M. Yaghi, *Proc. Natl. Acad. Sci. USA* **2006**, *103*, 10186–10191.
[10] J. J. Low, A. I. Benin, P. Jakubczak, J. F. Abrahamian, S. A. Faheem, R. R. Willis, *J. Am. Chem. Soc.* **2009**, *131*, 15834–15842.
[11] M. Tonigold, Y. Lu, A. Mavrandonakis, A. Puls, R. Staudt, J. Möllmer. J. Sauer, D. Volkmer, *Chem. Eur. J.* **2011**, *17*, 8671–8695.
[12] J. Y. Lee, O. K. Farha, J. Roberts, K. A. Scheidt, S. T. Nguyen, J. T. Hupp, *Chem. Soc. Rev.* **2009**, *38*, 1450–1459.
[13] C. Heering, I. Boldog, V. Vasylyeva, J. Sanchiz, C. Janiak, *CrystEngComm* **2013**, *15*, 9757–9768.
[14] B. J. Burnett, P. M. Barron, W. Choe, *CrystEngComm* **2012**, *14*, 3839–3846.
[15] M. Viciano-Chumillas, S. Tanase, L. J. de Jongh, J. Reedijk, *Eur. J. Inorg. Chem.* **2010**, *22*, 3403–3418.
[16] C. W. Lu, Y. Wang, Y. Chi, *Chem. Eur. J.* **2016**, *22*, 17892–17908.
[17] K. J. Gagnon, H. P. Perry, A. Clearfield, *Chem. Rev.* **2012**, *112*, 1034–1054.
[18] S. J. I. Shearan, N. Stock, F. Emmerling, J. Demel, P. A. Wright, K. D. Demadis, M. Vassaki, F. Costantino, R. Vivani, S. Sallard, I. R. Salcedo, A. Cabeza, M. Taddei, *Crystals* **2019**, *9*, 270.
[19] R. Silbernagel, C. H. Martin, A. Clearfield, *Inorg. Chem.* **2016**, *55*, 1651–1656.
[20] M. T. Wharmby, J. P. S. Mowat, S. P. Thompson, P. A. Wright, *J. Am. Chem. Soc.* **2011**, *133*, 1266–1269.
[21] T. Rhauderwiek, K. Wolkersdörfer, S. Øien-Ø degaard, K. P. Lillerud, M. Wark, N. Stock, *Chem. Commun.* **2018**, *54*, 389–392.
[22] T. Rhauderwiek, H. Zhao, P. Hirschle, M. Doeblinger, B. Bueken, H. Reinsch, D. D. Vos, S. Wuttke, U. Kolb, N. Stock, *Chem. Sci.* **2018**, *9*, 5467–5478.
[23] J. Jia, X. Lin, C. Wilson, A. J. Blake, N. R. Champness, P. Hubberstey, G. Walker, E. J. Cussen, M. Schroeder, *Chem. Commun.* **2007**, 840–842.
[24] X. J. Gu, Z. H. Lu, Q. Xu, *Chem. Commun.* **2010**, *46*, 7400–7402.
[25] T.–L. Ho, *Chem. Rev.* **1975**, *75*, 1–20.
[26] M. O'Keeffe, *Chem. Soc. Rev.* **2009**, *38*, 1215–1217.
[27] M. O'Keeffe, O. M. Yaghi, *Chem. Rev.* **2012**, *112*, 675–702.
[28] P. O. Adelani, L. J. Jouffret, J. E. S. Szymanowski, P. C. Burns, *Inorg. Chem.* **2012**, *51*, 12032–12040.
[29] P. O. Adelani, G. E. Sigmon, P. C. Burns, *Inorg. Chem.* **2013**, *52*, 6245–6247.
[30] J. Dechnik, A. Nuhnen, C. Janiak, *Cryst. Growth Des.* **2017**, *17*, 4090–4099.
[31] C. Heering, B. Francis, B. Nateghi, G. Makhloufi, S. Luedeke, C. Janiak, *CrystEngComm* **2016**, *18*, 5209–5223.
[32] J. Liu, R. Zeng, C. Zhou, J. Zou, *Chin. J. Chem.* **2011**, *29*, 309–313.
[33] A. Spassow, *Organic Syntheses* **1955**, *3*, 390.
[34] A. Sarkar, S. R. Roy, N. Parikh, A. K. Chakraborti, *J. Org. Chem.* **2011**, *76*, 7132–7140.
[35] T. Steiner, *Acta Crystallogr. B* **1998**, *54*, 456–463.
[36] J. Grell, J. Bernstein, G. Tinhofer, *Crystallogr. Rev.* **2002**, *8*, 1–56.
[37] I. Boldog, J. C. Daran, A. N. Chernega, E. B. Rusanov, H. Krautscheid, K. V. Domasevitch, *Cryst. Growth Des.* **2009**, *9*, 2895–2905.
[38] F. H. Allen, W. D. Samuel Motherwell, P. R. Raithby, G. P. Shields, R. Taylor, *New J. Chem.* **1999**, *23*, 25–34.
[39] T. Steiner, *Angew. Chem. Int. Ed.* **2002**, *41*, 48–76.
[40] S. Vairam, S. Govindarajan, *Thermochim. Acta* **2004**, *414*, 263–270.
[41] N. Miyaura, A. Suzuki, *Chem. Rev.* **1995**, *95*, 2457–2483.

[42] Apex2, Data Reduction and Frame Integration Program for the CCD Area-Detector System, Bruker AXS Inc., Madison, Wisconsin (USA) **1997–2006**.
[43] Smart, Saint, Area Detector Control and Integration Software, Bruker AXS Inc., Madison, Wisconsin (USA) **2003**.
[44] G. M. Sheldrick, Sadabs, Area-Detector Absorption Correction, University of Göttingen, Göttingen (Germany) **1996**.
[45] G. M. Sheldrick, *Acta Crystallogr*. **2015**, *A71*, 3–8.
[46] G. M. Sheldrick, *Acta Crystallogr*. **2008**, *A64*, 112–122.
[47] K. Brandenburg, Diamond (version 4.4), Crystal and Molecular Structure Visualization, Crystal Impact – K. Brandenburg & H. Putz Gbr, Bonn (Germany) **2009–2017**.

Supplementary Material: The online version of this article offers supplementary material (https://doi.org/10.1515/znb-2019-0170).